The Geological Society of America
Special Paper 452
2009

Evidence for a change in Milankovitch forcing caused by extraterrestrial events at Massignano, Italy, Eocene-Oligocene boundary GSSP

Rachel E. Brown*†
Carleton College, One North College Street, Northfield, Minnesota 55057, USA

Christian Koeberl†
Center of Earth Sciences, University of Vienna, Althanstrasse 14, A-1090 Vienna, Austria

Alessandro Montanari†
Osservatorio Geologico di Coldigioco, I-62020 Frontale di Apiro (MC), Italy,

David M. Bice†
The Pennsylvania State University, Department of Geosciences, 503 Deike Building, University Park, Pennsylvania 16802, USA

ABSTRACT

High-resolution spectral analyses of four climate proxies from Massignano, Italy (Eocene-Oligocene boundary global stratotype section and point [GSSP]) indicate that the deposition of this rhythmically bedded sedimentary sequence was controlled by Milankovitch orbital cycles. An inverse relationship between the magnetic susceptibility record and the co-varied calcium carbonate, $\delta^{18}O$, and $\delta^{13}C$ records is indicative of a climate model in which limestones represent dry/cold periods, while marly limestones represent warm/wet periods. Through pattern matching of band-pass filtered signals with the La2004 eccentricity curve, we propose an astrochronological calibration for this important time period. Constrained by three radioisotopically dated volcanic ashes and based on a band-pass version of eccentricity that exhibits expected amplitude modulations, our astrochronology yields a refined age for the Eocene-Oligocene boundary of 33.91 ± 0.05 Ma. Orbital forcing is less pronounced in the lower portion of the Massignano section (meter levels 0–15), which contains evidence of several impact events and a 2.2-m.y.-long comet/asteroid shower. We propose that substantial, nonperiodic climate alterations caused by this period of enhanced extraterrestrial activity mask the Milankovitch climate cycles. Possible mechanisms for the exaggeration of impact-related climatic changes include the ice-albedo feedback or the combined effect of impact-related atmospheric alterations with ongoing dust-particle loading associated with the comet/asteroid shower.

Keywords: Eocene/Oligocene boundary, Milankovitch theory, impacts, spectral analysis, stable isotopes.

*Corresponding author. Present address: University of California, Santa Cruz, 1156 High Street, Santa Cruz, California 95064, USA.
†E-mails: brown@pmc.ucsc.edu; christian.koeberl@univie.ac.at; sandro.ogc@fastnet.it; dbice@geosc.psu.edu.

Brown, R.E., Koeberl, C., Montanari, A., and Bice, D.M., 2009, Evidence for a change in Milankovitch forcing caused by extraterrestrial events at Massignano, Italy, Eocene-Oligocene boundary GSSP, *in* Koeberl, C., and Montanari, A., eds., The Late Eocene Earth—Hothouse, Icehouse, and Impacts: Geological Society of America Special Paper 452, p. 1–19, doi: 10.1130/2009.2452(08).

INTRODUCTION

The mid- to late Eocene is characterized by accelerated global cooling coincident with the appearance of Antarctic polar ice sheets (Fig. 1) (e.g., Prothero, 1994; Zachos et al., 1994, 2001; Zanazzi et al., 2007). This long-term climate cooling trend is reflected by an increase in marine oxygen isotope values (e.g., Mackensen and Ehrmann, 1992; Zachos et al., 1994), an ~55 m sea-level fall (Miller et al., 2008), and the occurrence of significant biotic turnovers (Berggren and Prothero, 1992). The cooling trend, however, is further complicated by the occurrence of multiple bolide impact events (e.g., Glass and Koeberl, 1999; Montanari and Koeberl, 2000; Deutsch and Koeberl, 2006), including the nearly contemporaneous Chesapeake Bay and Popigai impacts. These and other impact events, which are possibly related to an extensive late Eocene comet shower (Farley et al., 1998) or asteroid shower (Tagle and Claeys, 2004), may also have had a significant impact on global climate (Vonhof et al., 2000; Bodiselitsch et al., 2004).

The pelagic sediments of the Umbria-Marche Basin, Italy, which were deposited during the period of Eocene-Oligocene cooling, provide insight into the manner in which local sedimentation and regional climate patterns were affected by both ice-sheet development and impact events. The 23-m-thick sequence of pelagic limestone and marly limestone exposed at the Massignano Quarry (global stratotype section and point [GSSP] for the Eocene-Oligocene boundary), located in the easternmost part of the basin (Fig. 2), is ideal for cyclostratigraphic analysis, as it is both continuous and undisturbed (Cotillion, 1995). Moreover, the sequence contains three radioisotopically dated volcanic ashes (Montanari et al., 1988, 1993; Montanari and Koeberl, 2000, and references therein), which provide time constraints for the section and allow for correlation between the stratigraphic climate record and mathematically predicted orbital variations (e.g., Laskar et al., 2004).

In this study, we analyzed four different high-resolution climate proxies in the Massignano section, including carbonate content, magnetic susceptibility, and bulk-rock oxygen and carbon stable isotopes, in order to provide insight into orbital forcing on the Eocene-Oligocene climate system and determine precise astrochronological ages for stratigraphic horizons.

GEOLOGIC SETTING

The Massignano section (43°32′13″N; 13°35′36″E; Jovane et al., 2007), which became the GSSP for the Eocene-Oligocene boundary in 1993 (Premoli-Silva and Jenkins, 1993), consists of 23 m of alternating pale green- and pink-colored pelagic limestones and marly limestones (Fig. 3). As part of

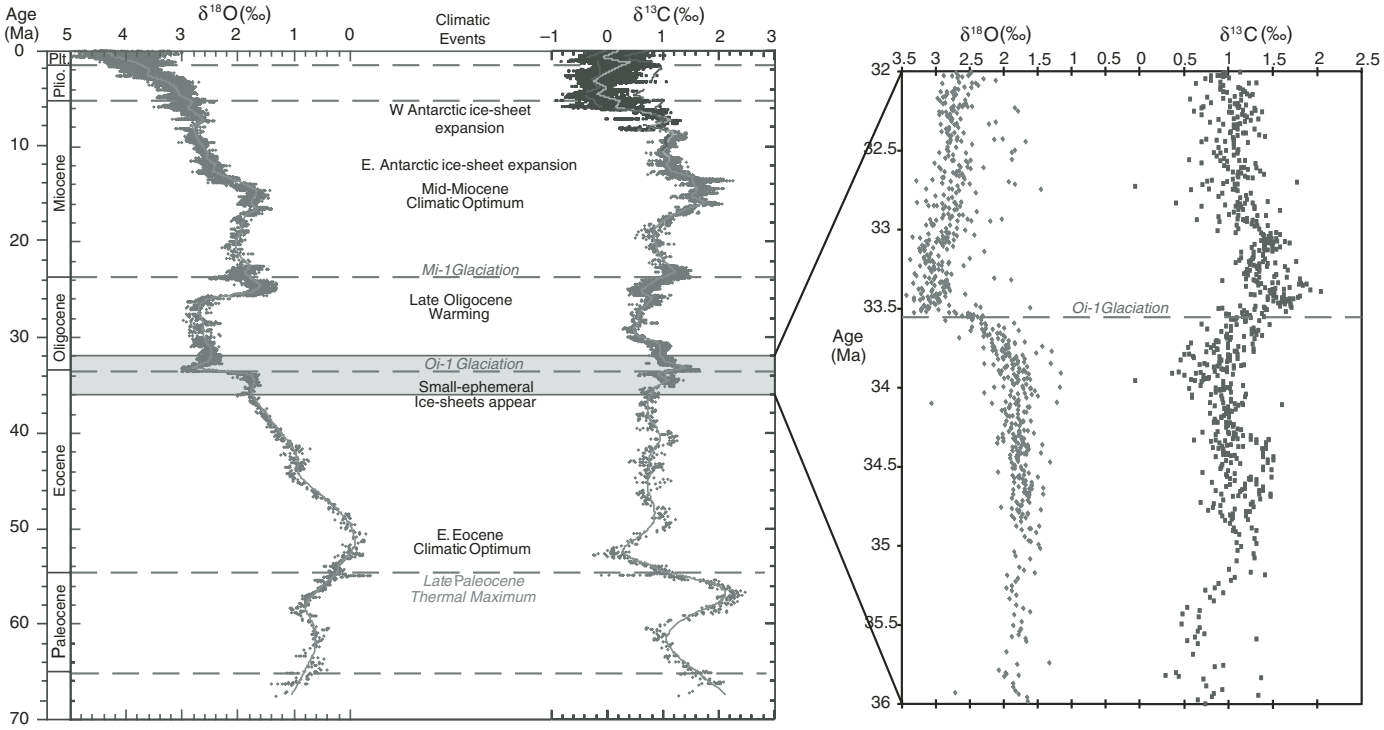

Figure 1. Global deep-sea carbon and oxygen isotope records compiled from pelagic sediments at over 40 Deep Sea Drilling Project (DSDP) and Ocean Drilling Program (ODP) sites. The ^{18}O trends reflect changes in global ice volume and temperature, while ^{13}C trends are primarily indicative of changes in productivity. The section of interest between 32 and 36 Ma, outlined by the gray box at the left, is isolated on the right. Note the change in scale in the inset (after Zachos et al., 2001). The abbreviations in the upper left hand corner are for Pliocene and Pleistocene.

the Umbria-Marche sedimentary basin (paleolatitude ~34°N; Dercourt et al., 1993), the sequence was deposited in the Neotethys Ocean at a paleodepth of ~1000–1500 m (Coccioni and Galeotti, 2003). The section contains two distinctive formations, the Scaglia Variegata Formation and Scaglia Cinerea Formation, which span an interval from the latest Eocene to early Oligocene (e.g., Lowrie and Lanci, 1994).

As the type section for the Eocene-Oligocene boundary, Massignano has been the subject of a number of detailed studies integrating litho-, bio-, magneto-, and chemostratigraphy (see, e.g., Premoli-Silva et al., 1988, Montanari and Koeberl, 2000, Jovane at el., 2004, and references therein). Three radioisotopically dated biotite-rich volcano-sedimentary layers are found at meter levels 7.2, 12.7, and 14.7, and they provide independent age constraints necessary for compelling astronomical dating (Montanari et al., 1988; Montanari et al., 1993; Montanari and Koeberl, 2000, and references therein). Montanari et al. (1993) reported revised mean ages of 35.4 ± 0.3 Ma, 34.5 ± 0.3 Ma, and 34.2 ± 0.2 Ma for these three layers, respectively. In addition, the section contains several other biotite-rich volcano-sedimentary layers as well as impactoclastic layers marked by Ir anomalies (Montanari et al., 1988, 1993), shocked quartz grains (Clymer et al., 1996; Langenhorst, 1996), and finally, a broad ^{3}He anomaly (Farley et al., 1998), which has been interpreted as evidence for a comet shower lasting ~2.2 m.y.

FIELD AND LABORATORY METHODS

Sample Collection

Following the work of Coccioni et al. (1988), we relogged the Massignano section and sampled between meter levels 0.5 and 23 at a 5 cm sampling resolution (Fig. 3). The section is heavily bioturbated (Huber et al., 2001), making a higher sampling resolution inadvisable. Samples weighing a minimum of 20 g were primarily collected using a Bosch PbH 200 RE masonry drill with a 12 mm drill bit. Marly layers not conducive to drilling were collected as hand samples. Samples were dried, powdered (using a brass mortar and pestle), and sieved to a grain size of 1–2 mm to ensure homogeneity.

Figure 2. Location map of the Massignano section, Marche region, Italy. Landsat image in the upper right is courtesy of the Global Land Cover Facility.

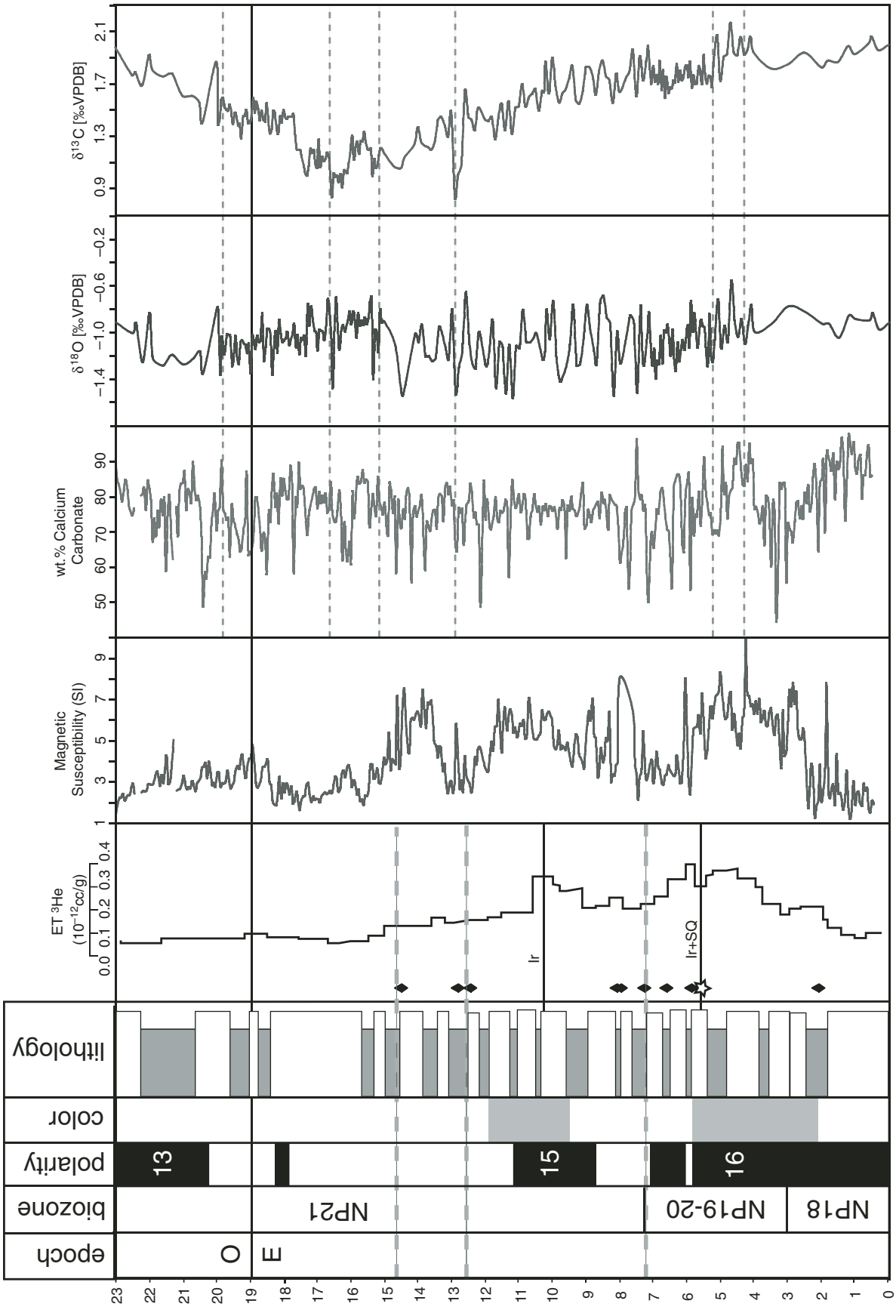

Figure 3. Lithostratigraphy, ^{3}He content (Farley et al., 1998), magnetic susceptibility, carbonate content, and oxygen and carbon stable isotope records (this study; Bodiselitsch et al., 2004) from the Massignano section. The Eocene-Oligocene boundary is located at meter level 19. The dark boxes under "color" represent reddish intervals, horizontal dashed lines denote dated volcanic ashes (Montanari et al., 1988), diamonds signify biotite-rich layers, and the star is indicative of shocked quartz (Clymer et al., 1996). Note that the carbonate content co-varies with the isotope data but exhibits a primarily inverse relationship with magnetic susceptibility. Ashes have been removed from the magnetic susceptibility record to accentuate variability. See Premoli-Silva et al. (1988) and references therein for further information on the biozones and magnetic polarity. E—Eocene; O—Oligocene; VPDB—Vienna Peedee belemnite.

Percent Carbonate and Magnetic Susceptibility

The carbonate content determinations and magnetic susceptibility analyses were completed at the Osservatorio Geologico di Coldigioco. We measured the calcium carbonate content using a Dietrich-Fruling water calcimeter with ±2 rel% precision. Samples weighing between 300 and 320 mg (and powdered to a grain size < 250 μm) were reacted in excess with a 10 vol% HCl in water solution for 2 min. Standards (Carrara marble) were run after every 20 samples to ensure proper calibration.

Mass specific magnetic susceptibility measurements were carried out on a Bartington MS2 and a Bartington MS2B dual-frequency sensor on low frequency (0.465 kHz) and ×0.1 sensitivity. Samples were measured at a constant volume, and their masses were noted. Air measurements were made between samples to correct for thermally induced drift.

Bulk-Rock Stable Isotopes

Oxygen and carbon stable isotopic compositions were obtained from bulk-rock carbonate at 5 cm intervals in two short intervals of the Massignano section: meter levels 5.25–7.1 and 15–20 (Fig. 3). The first of these intervals contains an impactoclastic layer at meter level 5.6, and a small iridium anomaly at meter level 6.2 (Montanari et al., 1993; Bodiselitsch et al., 2004), while the second contains the Eocene-Oligocene boundary at meter level 19. Stable isotope analyses were carried out at Pennsylvania State University on a Finnigan MAT 252 isotope-ratio mass spectrometer with common acid bath. Samples were reacted in 100% anhydrous phosphoric acid at 90 °C. The isotope data are reported in per mil deviations from the international Vienna Peedee belemnite (V-PDB) carbonate standard, to which the data have been calibrated with NBS-19. Analytical precision for $\delta^{18}O$ and $\delta^{13}C$ values is 0.1‰ and 0.07‰, respectively.

The use of bulk carbonates in stable isotope analysis is convenient because it requires very small amounts of sample material and also allows for the rapid analysis of numerous samples. One concern with this method, however, is that, because the bulk samples represent a mixture of carbonates from different sources, the $\delta^{18}O$ of seawater will not be accurately represented (Stoll and Schrag, 2000). While this concern is valid, comparisons of single species foraminiferal $\delta^{18}O$ records with those of bulk carbonates show that bulk carbonates do in fact accurately represent changes in both sea-surface temperature and the $\delta^{18}O$ of seawater when environmental changes are universal, affecting species throughout the water column (Shackleton et al., 1993; Schrag et al., 1995). Another potential problem with using bulk carbonates is that weathering and diagenesis may alter the original carbon and oxygen isotopic compositions (Banner and Hanson, 1990). Weathering at Massignano is minimized, since the excavation of the quarry front was discontinued some 30 yr ago, and the outcrop is now maintained by the Monte Cònero Regional Park. Furthermore, Odin et al. (1988) found no evidence of carbonate recrystallization at Massignano, though scanning electron microscope (SEM) analysis has revealed that foraminifers from the section contain secondary, blocky calcite (Vonhof et al., 2000). Still, as long as sediments in the same section experience recrystallization at the same rate through time, they will contain about the same amount of secondary calcite. The mean $\delta^{18}O$ values may be shifted in either direction, but the important primary variations are preserved (Stoll and Schrag, 2000).

Spectral Analysis

We conducted spectral analyses of the four proxy data sets in Matlab 5.2 using algorithms modified from Muller and MacDonald (2000). Outliers, namely ash deposits with anomalously high magnetic susceptibility values, were removed from the data set, requiring linear interpolation between points. We then performed fast Fourier transforms (FFTs) of the data (detrended and padded with zeros) in the stratigraphic domain, which yielded a set of spectral peaks representing cycles per stratigraphic centimeter. The spectral power used here is the complex conjugate of the Fourier coefficients normalized to unit mean power (Muller and MacDonald, 2000). We evaluated the statistical significance of the spectral peaks by generating a 95% confidence level from a Monte Carlo noise simulation (Muller and MacDonald, 2000). In this approach, 1000 random number sets with the same dimensions as the data are generated and then run through a FFT to find spectral power at each frequency. The 95% confidence level was estimated from these 1000 spectral results by calculating the mean value for each frequency three times. Peaks rising above this 95% confidence level were considered to be statistically significant. We assume that prominent, statistically significant peaks in the magnetic susceptibility data that are related to one another by the same ratios found between Milankovitch cycles represent eccentricity, obliquity, and precession, making it possible to correlate meter level to age through the calculation of an average sedimentation rate. For the Massignano section, we calculated an average sedimentation rate of 10.6 m/m.y., which is consistent with the possible range of sedimentation rates suggested by the independently dated volcanic ashes (between 4.4 m/m.y. and 10.8 m/m.y. using the revised ash dates reported by Montanari et al., 1993), and it is in agreement with sedimentation rates suggested by magnetostratigraphy (Lowrie and Lanci, 1994). The 23 m section, therefore, spans a time period of 2.17 m.y., with an average time interval of 4.72 k.y. between samples (every 5 cm). Spectral peaks with periods greater than ~800 k.y. are therefore not significant in the Massignano section, as they were repeated fewer than three times during deposition.

Amplitude modulations were evaluated for both the mathematically predicted orbital cycles as well as for the cycles in our $CaCO_3$ content data following the approach of Grippo et al. (2004) and Mitchell et al. (2008). This analysis provides a means for testing the hypothesis that the Milankovitch-band cycles are indeed orbital cycles—if they are, then we expect them to have

the predicted amplitude modulations. The first step of this process involved isolating the presumed orbital signals from the raw data using Gaussian band-pass filters (eccentricity, 145–75 k.y.; obliquity, 50–35 k.y.; and precession, 25–17 k.y.). We then applied a Hilbert transform to each of the presumed orbital signals, which resulted in an enveloping curve that graphically illustrates the amplitude modulation. We then applied a FFT to this enveloping curve in order to identify the spectral character of the amplitude modulation. A similar amplitude modulation analysis of the Laskar 2004 (La2004) orbital parameters allowed us to compare our presumed orbital signals with the mathematically predicted cycles.

To examine the stratigraphic changes in spectral power, the result of likely variations in environmental conditions and sediment accumulation rates, we employed a sliding-window technique, or evolutionary spectral analysis, in which FFTs were performed on a specified portion or "window" of the data that shifted incrementally through the time series. By looking at the continuity of peaks through time, we can establish whether they represent long-term cyclicity or whether they are the result of random variations and climatic noise (Muller and MacDonald, 2000). Because the choice of window size can affect which cycles appear important, we used a variety of window sizes for the analysis and noted which frequencies were present, at least in part, in multiple windows. Frequencies observed in a range of window sizes and that were continuous through time are considered to reflect actual cyclic trends in the data. Prior to the sliding-window analyses, we applied broad band-pass filters to smooth the data, thereby removing long-period, low-frequency contributions that may be swamping the higher-frequency signals.

Astronomical dating was similarly accomplished through the use of broad band-pass filtering. Variations in the carbonate and magnetic susceptibility data between 140 and 85 k.y. were isolated so as to emphasize the variance in the short eccentricity band. These filtered data were then used for correlation via constrained pattern matching with the La2004 theoretical eccentricity curve of Laskar et al. (2004). The uncertainties in astronomical dating depend on (1) the astronomical solution applied; (2) the assumption of a constant sedimentation rate; and (3) the assumption that there is no lag between orbital forcing and its sedimentary expression (Kuiper et al., 2008). Laskar et al. (2004) estimated a maximum error in their calculations of 30 k.y. over the last 50 m.y. If we assume our tuning to be correct, then the error in the astronomical dates will be about half of the cycle period to which we are matching (short eccentricity), so for this study, about ±50 k.y.

RESULTS

Percent Carbonate and Magnetic Susceptibility Data

The carbonate content (% by weight $CaCO_3$) of the limestones and marly limestones of the Massignano section varies from 47.4 wt% to 96.1 wt%, with a mean of 76.9 wt% (Fig. 3). There is no trend through the section. Conversely, the magnetic susceptibility data exhibit an upsection trend of decreasing variability when the anomalously high ash-layer values are disregarded (Fig. 3). The magnetic susceptibility values fluctuate between 1.42 and 123 (SI units), averaging 4.72 SI. The highest values fall within the ash layers. Both proxy curves correspond well with lithology. The two data sets are inversely related, such that high carbonate percentages correspond with low magnetic susceptibility values.

Bulk-Rock Stable Isotope Data

The oxygen and carbon isotopic data (Fig. 3) from this study, combined with those of Bodiselitsch et al. (2004), correlate well with lithology and appear to co-vary, such that $\delta^{18}O$ highs correspond with $\delta^{13}C$ highs, though this relationship is less clear in the lower section. A decreasing trend is visible in the $\delta^{13}C$ data through the majority of the section, followed by an increasing trend from about meter-level 17 to the top. The $\delta^{13}C$ values from the lower high-resolution interval (5.35–7.10 m) fluctuate between 1.53‰ and 1.83‰ (averaging 1.7‰), while values in the upper section (m 15–20) range from 0.8‰ to 1.6‰ (with an average of 1.28‰) and exhibit a marked upsection increase.

Trends in the $\delta^{18}O$ data are less pronounced, but there appears to be a general decrease in values from meter level 3 to 8, followed by an increase and a subsequent decrease from about meter level 15 to 21. For meters 15–20, the $\delta^{18}O$ values range from –0.73‰ to –1.51‰ (averaging −1.05‰). Values are similar between meters 5.35 and 7.10, varying from –0.84‰ and –1.43‰ (averaging −1.16‰).

In comparison with the global benthic foraminiferal $\delta^{18}O$ values listed in Figure 1, we can see that the isotope values are on the heavier side. The $\delta^{18}O$ values reported in this study average about −1‰ as opposed to an average of about −2‰ in the global benthic compilation for this time period. Similarly, the $\delta^{13}C$ values from this study average ~1.5‰, rather than 1‰. These differences likely result from two sources: (1) in this study, we used bulk-rock stable isotopes rather than isotopes from benthic foraminifera, and (2) the paleolatitude of the study site is ~34°N (Dercourt et al., 1993), and so it is a lower-latitude site where temperatures and rates of productivity are generally higher.

Notably, the significant positive isotope excursion that marks the Eocene-Oligocene boundary in the global benthic record (Fig. 1) is lacking at Massignano. Both the $\delta^{18}O$ and $\delta^{13}C$ isotope records do, however, begin to show a slight increase in values near the top of the record. The $\delta^{13}C$ record begins to increase slightly before the boundary at about meter level 17, while the $\delta^{18}O$ record does not begin to increase until after the boundary at about meter level 21. It may be that only the beginning of the first step of the two-step Eocene-Oligocene transition proposed by Coxall et al. (2005) is preserved at Massignano, as the section ends just a few meters above the Eocene-Oligocene boundary, and the more dramatic second step is not preserved here.

Spectral Analysis

Fast Fourier Transform

Spectral analysis results for the percent carbonate and magnetic susceptibility data (Fig. 4) were obtained using a linear sedimentation rate of 10.6 m/m.y., which was calculated by matching peaks in the meter-level domain to known astronomical cycles. The plots are quite noisy, particularly that for the $CaCO_3$ content, and while orbital peaks are present, they do not all emerge significantly above the noise level. Prominent spectral power peaks for the $CaCO_3$ content occur at 315, 60, 41, 30, and 24 k.y., and for magnetic susceptibility, peaks occur at 254, 116, 43, and 24 k.y., all of which exceed the 95% confidence limit.

Knowledge of the comet shower and multiple volcanic ashes in the lower and central portion of the section prompted a split analysis of the outcrop. The results for the split section are shown in Figures 5 and 6. The plots for the upper portion (meters 15–23) are considerably less noisy. Common elements to all four proxies include a peak or cluster of peaks at 36–43 k.y., and pronounced peaks at 95 or 97, as well as at 23–25 k.y. Both the magnetic susceptibility and $CaCO_3$ content plots exhibit strong peaks at ~125–127 k.y. and ~95–97 k.y. This second peak is also notable in the plot for $\delta^{13}C$, while the peaks with the greatest spectral power in $\delta^{18}O$ plot are those at 23 and 19 k.y. Spectral peaks with periods greater than 250 k.y. are not considered significant, as the section under scrutiny spans just 755 k.y. Although neither rises above the 95% confidence interval, a peak at 55 k.y. is prominent in three of the records, as is a peak at 30 or 31 k.y. A 55 k.y. peak may reflect either the 54 k.y. obliquity component or the first harmonic of the 100 k.y. eccentricity (F. Hilgen, 2008, personal commun.). According to Mix et al. (1995), a 29–31 k.y. peak may be caused by nonlinear coupling of eccentricity and obliquity; however, in this case, a strong 41 k.y. obliquity component would also be expected. Alternatively, a 29–31 k.y. peak could be explained by the combination of precession components, or of precession and obliquity (von Dobeneck and Schmieder, 1999).

The spectral plots for the lower portion are reminiscent of the whole-section plots, exhibiting an elevated level of noise (Fig. 6). The most prominent peaks in the magnetic susceptibility and $CaCO_3$ data that are possibly orbital in origin are at 44 and 24 k.y. A peak seen in the $CaCO_3$ data at 58 k.y. is not echoed in the magnetic susceptibility record. In the $\delta^{13}C$ record, peaks at 245 and 150 k.y. are the only ones to rise above the 95% confidence interval, though peaks at 123, 86, and 56 k.y. all seem to stand out from the rest. Finally, in the $\delta^{18}O$ record, prominent peaks at 144, 77, 22, and 18 k.y. appear significant.

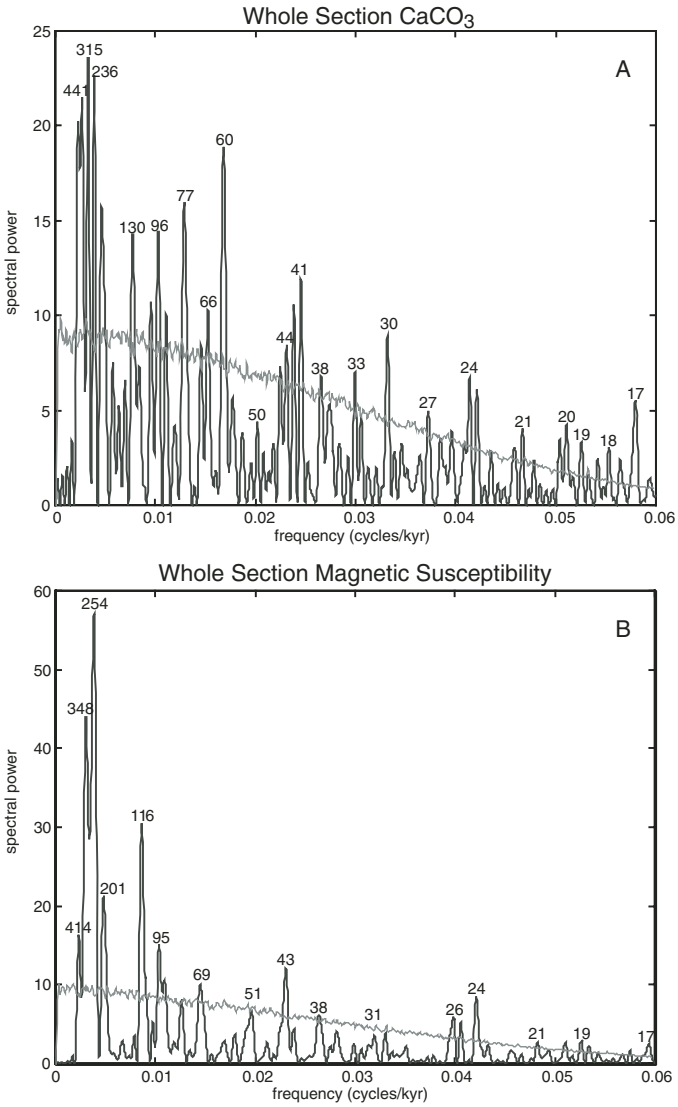

Figure 4. Spectral analysis results for (A) $CaCO_3$ content and (B) magnetic susceptibility for the entire Massignano section using a sedimentation rate of 10.6 m/m.y. and 10–700 k.y. band-pass filter to remove long-period, low-frequency contributions. The black curve (with peaks labeled in k.y.) represents the various cycles present in the data. The light-gray line is the 95% confidence limit; peaks rising above this curve can be attributed to true cyclicity with 95% confidence. While orbital peaks are present, other peaks appear equally or even more pronounced.

Amplitude Modulations

Amplitude modulations, which reflect a beat between fundamental astronomical frequencies, are not easily introduced into a data set via the tuning process (Pälike et al., 2001) and can, therefore, provide insight into how strongly an astronomical forcing is represented in the data (Laskar, 1999). Amplitude modulations often cited in the literature include the 400 k.y. modulation of climatic precession by eccentricity, as well as the 1.2 m.y. obliquity modulation (e.g., Lourens and Hilgen, 1997; Turco et al., 2001; Grippo et al., 2004; Pälike et al., 2004). All three of the spectral plots displaying amplitude modulations of the Massignano percent carbonate display amplitude modulation peaks that are in agreement with the peaks expected from the mathematically predicted Laskar et al. (2004) curve (Fig. 7). The amplitude modulations exhibited by the Massignano percent carbonate short

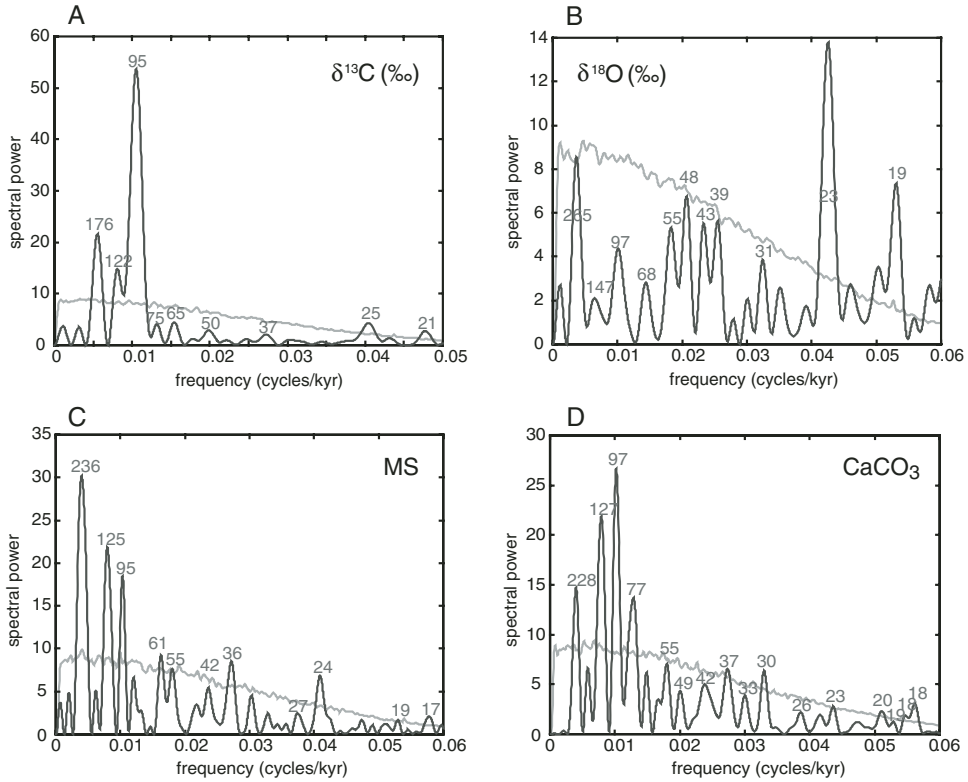

Figure 5. Spectral analysis results for (A) carbon isotopes, (B) oxygen isotopes, (C) magnetic susceptibility (MS), and (D) calcium carbonate content for the upper portion (meters 15–23) at Massignano, Italy. Data from Bodiselitsch et al. (2004) were combined with data from this study to produce the carbon and oxygen stable isotope plots. Again, the black curve with peaks labeled in k.y. represents the cycles present in the data, while the light-gray curve is the 95% confidence limit. These plots are considerably less noisy than those for the whole section. Common elements in the four plots include a peak or peak cluster at 36–43 k.y., and pronounced peaks at 95 or 97 k.y., as well as at 23–25 k.y. Both the eccentricity and precession peaks consistently clear the light-gray 95% confidence line; however, the obliquity peak does not.

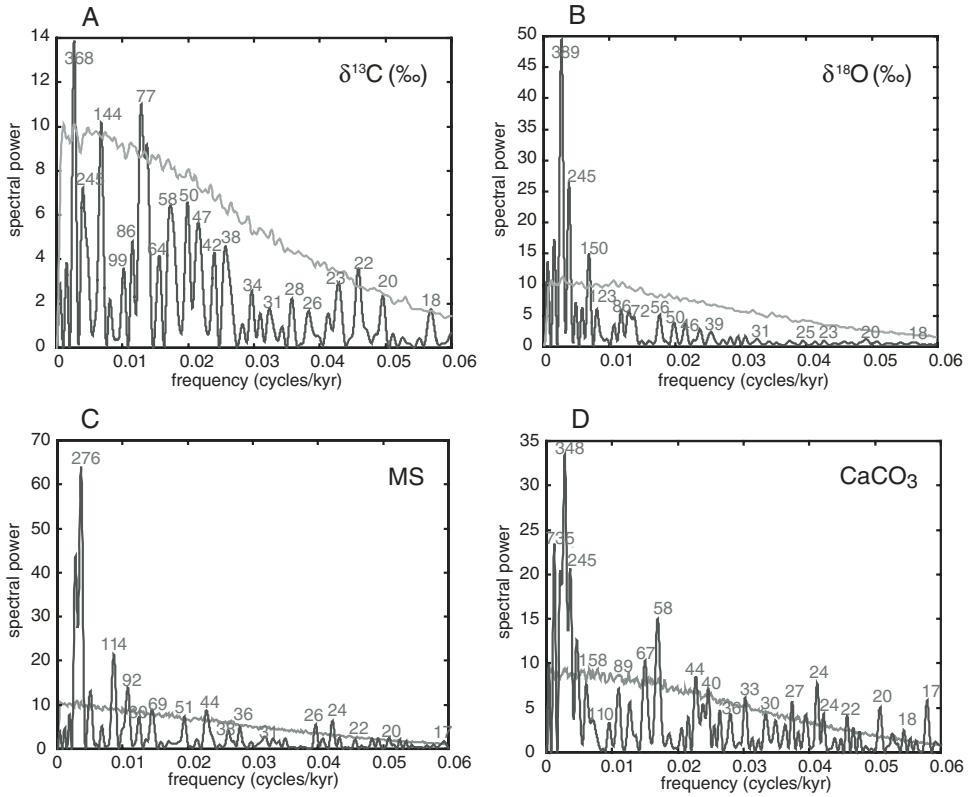

Figure 6. Spectral analysis results for all four proxies in the lower portion (meters 0.5–15) of the Massignano section: (A) carbon isotopes, (B) oxygen isotopes, (C) magnetic susceptibility (MS), and (D) calcium carbonate content. Data from Bodiselitsch et al. (2004) were combined with data from this study to produce the carbon and oxygen stable isotope plots. The black curve represents the various cycles present in the data, and the light-gray line is the 95% confidence limit. Cycles are labeled in k.y. Similar to the spectral plots for the entire section, these plots exhibit a significant amount of noise.

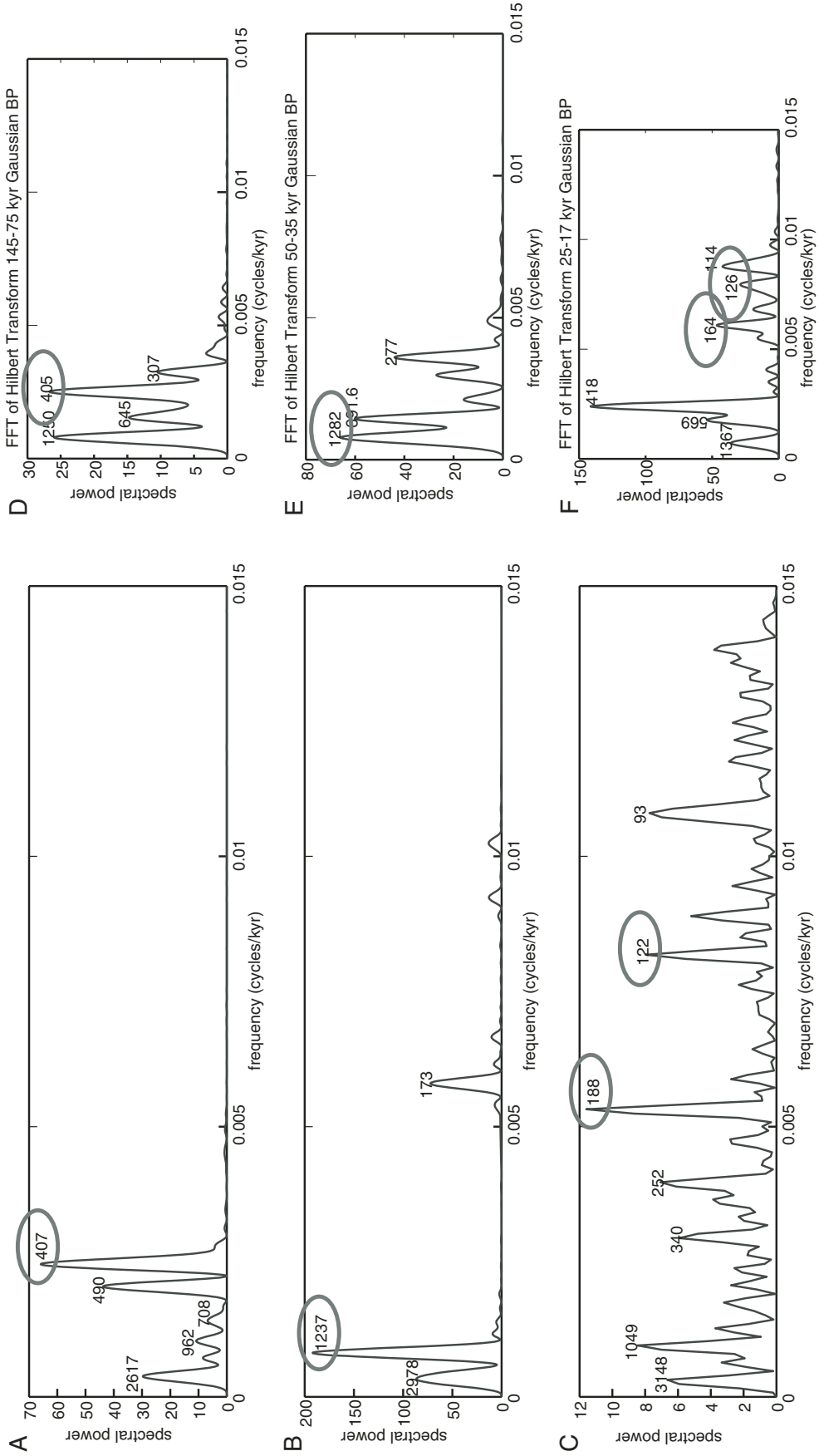

Figure 7. Amplitude modulations of Laskar et al. (2004) for (A) short eccentricity, (B) obliquity, and (C) precession, as well as of the Massignano section calcium carbonate (D) short eccentricity, (E) obliquity, and (F) precession signals. These plots were obtained following the approach of Grippo et al. (2004). We employed a Hilbert transform to find the enveloping curve of a Gaussian band-passed (BP) signal followed by a fast Fourier transform (FFT) of the enveloping curve. Notable and consistent amplitude modulations are denoted by the gray ovals.

eccentricity signal include a 405 k.y. peak, as well as peaks at 1250, 645, and 307 k.y. For the obliquity signal, the most prominent peak has a period of ~1.2 m.y., with two other peaks at ~692 and 277 k.y. Finally, amplitude modulations of the precessional signal include a conspicuous peak with a period of ~418 k.y., as well as peaks at ~569, 164, 114, 126, and 1367 k.y.

Evolutionary Spectral Analyses

In the upper section, by comparing results from sliding-window analyses using both medium and small window sizes, it is apparent that long-term cyclic variations are most prevalent in the $CaCO_3$, magnetic susceptibility, and $\delta^{13}C$ data. While all four proxies exhibit coherent spectral peaks in the medium-sized windows (200–400 k.y.) (Fig. 8), continuous, low-frequency, ~95–118 k.y. peaks are also evident in the $CaCO_3$, magnetic susceptibility, and $\delta^{13}C$ data in the smaller windows (100–226 k.y.) (Fig. 9). Furthermore, faintly continuous peaks are also visible at ~38–42 k.y. and 23–26 k.y. The peaks within the $\delta^{18}O$ data appear primarily discontinuous in the smaller window. Despite this, because three of the proxy records display coherent spectral peaks in multiple window sizes, it is reasonable to assert that the cyclicity apparent from the initial spectral analyses is not a result of random depositional variations, but of repeated climatic or depositional cycles.

DISCUSSION

Magnetic Susceptibility

Variability within the magnetic susceptibility record of a particular rock sequence can be explained in a number of ways. For one, hematite records a much lower magnetic susceptibil-

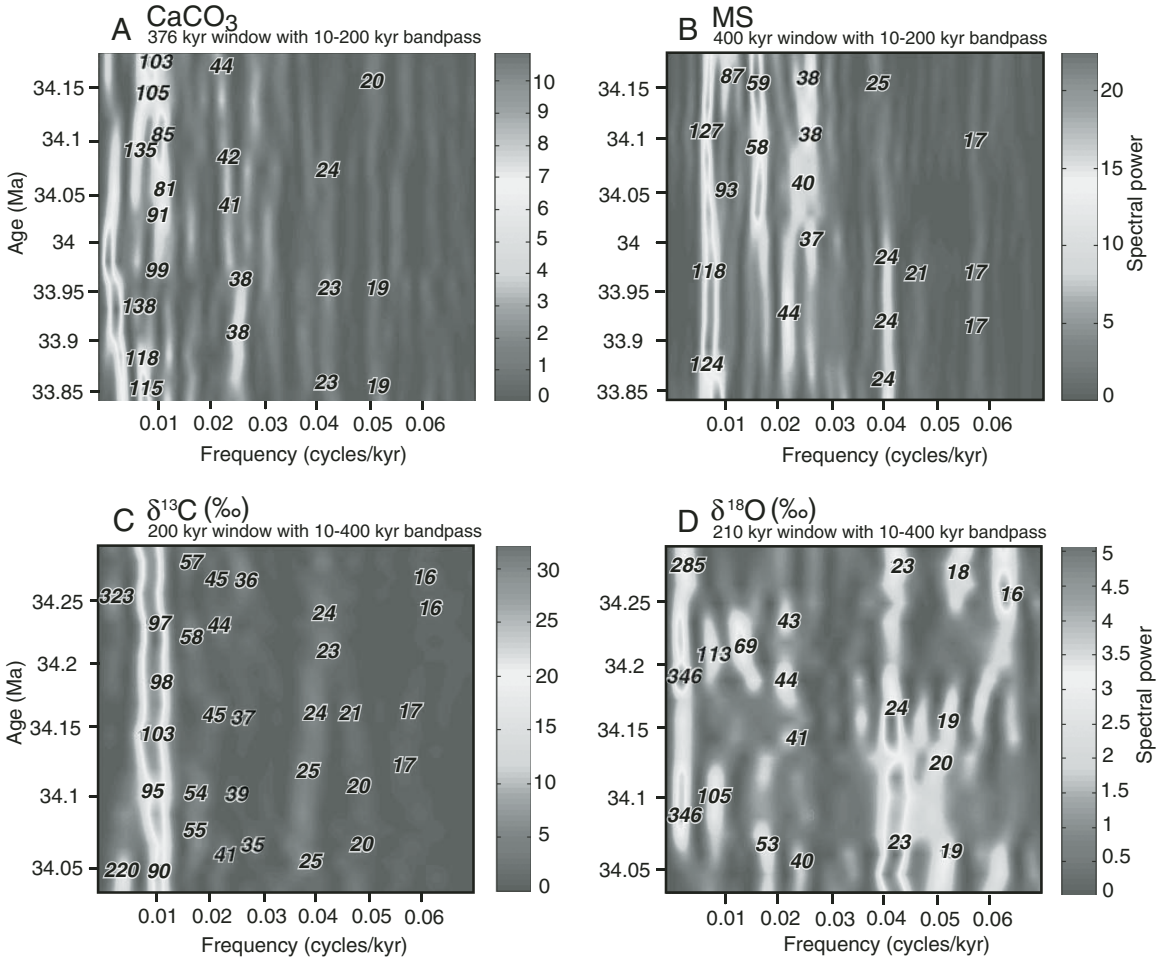

Figure 8. Results for the upper section from the medium-sized sliding-window spectral analyses, which are used to reveal changes in the spectral power of different frequencies over time from: (A) carbonate content (m 15–23), (B) magnetic susceptibility (m 15–23), (C) $\delta^{13}C$ (m 15–20), and (D) $\delta^{18}O$ (m 15–20). A medium-sized window is between two-fifths to one-half of the time scale in question, in this case, ~750 k.y. for plots A and B and ~470 k.y. for plots C and D. Spectral power scales are displayed to the right of each plot. The *y*-axis represents age in millions of years of the sliding-window midpoints.

ity value than magnetite, so a change in magnetic susceptibility could be illustrating a change in mineralogy. While the Massignano section does exhibit packages of reddish-tinted sediments, possibly indicative of elevated hematite content, these sections do not correspond with relatively lower magnetic susceptibility values. Contrarily, the reddish interval between meter levels 2 and 5 exhibits magnetic susceptibility values that are elevated in comparison with the rest of the sequence (Fig. 3). An alternate explanation hinges on terrigenous input, the primary source of iron-bearing minerals in pelagic sediments. Magnetic susceptibility variations are also thought to reflect variations in weathering and erosion caused by sea-level fluctuation or alterations in wet/dry climate cycling (Ellwood et al., 2000; Mader et al., 2004). Changes in sea level affect the supply of detrital material to the marine environment, as drops in base level associated with regressive periods enhance continental erosion (Crick et al., 1997). The variability in the magnetic susceptibility signal of the Massignano section could be linked to either climatically controlled continental erosion or, conversely, to variations in biogenic carbonate production, which would dilute an otherwise constant sediment supply.

Percent Carbonate and Stable Isotopes

Percent carbonate highs represent periods of increased carbonate production, decreased carbonate dissolution, or periods in which a steady supply of carbonate is periodically less diluted by fluxes in terrigenous input (Einsele and Ricken, 1991). Insight into which interpretation of calcium carbonate highs might best fit the Massignano section can be found by comparing the calcium carbonate content with the stable isotope data. At Massignano, there is a generally persistent covariance in the $CaCO_3$, $\delta^{13}C$, and $\delta^{18}O$ records (Fig. 3), which implies that the fluctuation in these parameters might be linked to a common paleoenvironmental cause. High carbonate accumulation corresponds to high planktonic productivity, evidenced by heightened $\delta^{13}C$ values

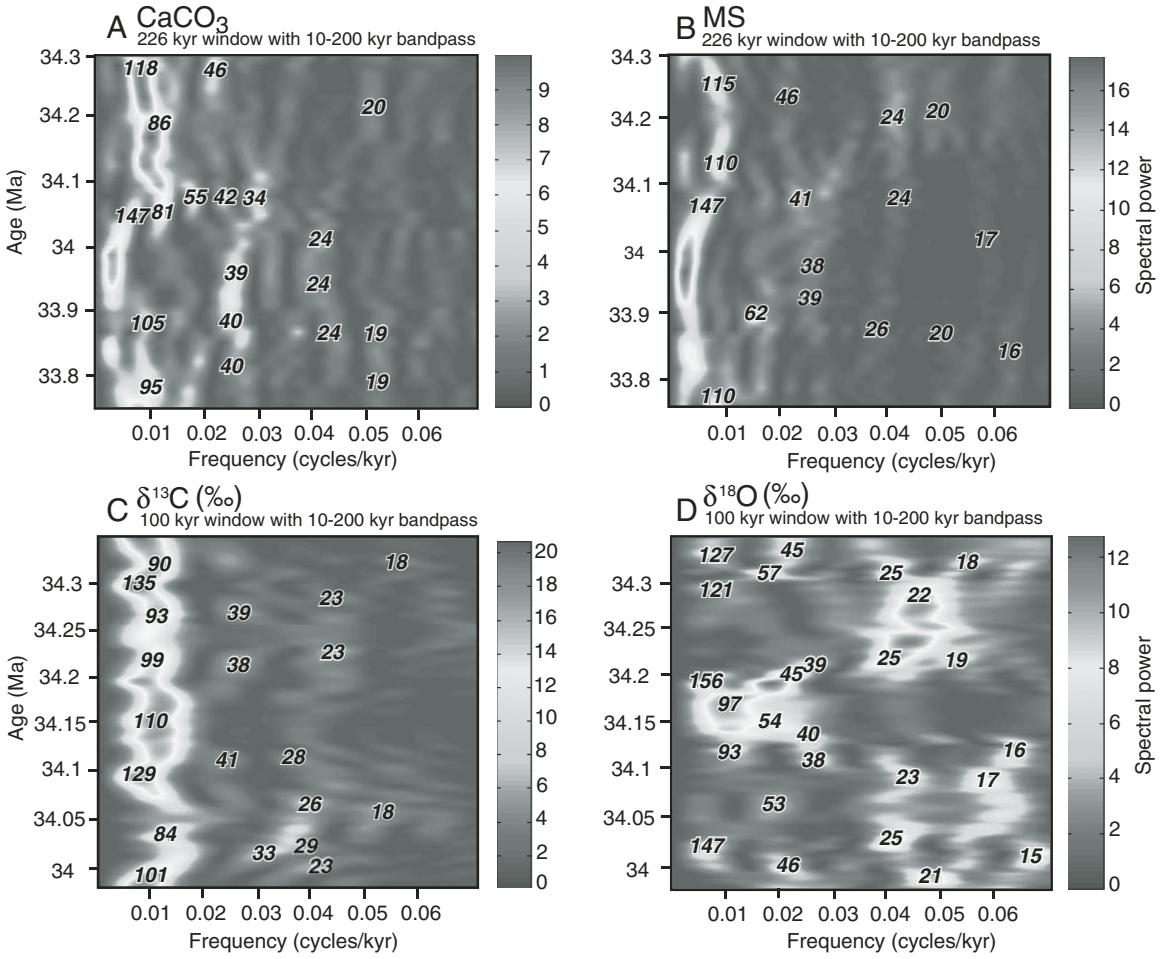

Figure 9. Results for the upper section from the small-sized sliding-window spectral analyses, which are used to reveal changes in the spectral power of different frequencies over time. Small-sized windows range between one-third and one-sixth of the time scale in question (100–226 k.y.). Spectral power scales are displayed to the right of each graph. Relatively continuous, low-frequency ~95–118 k.y. peaks are evident in the CaCO3, magnetic susceptibility, and $\delta^{13}C$ data.

resulting from the preferential fractionation of oceanic ^{12}C by marine photosynthesizers (Bickert, 2000). High carbonate accumulation is simultaneously matched with increased $\delta^{18}O$ values, implying high salinity conditions or low water temperatures at the time of limestone deposition. Following Mader et al. (2004) and in agreement with Jovane et al. (2006), we interpret the correspondence of stable isotope highs with high carbonate contents as an indication that Eocene-Oligocene Mediterranean limestone formation occurred during dry, cold periods marked by higher productivity. It is likely that increased ice volume and the appearance of small ephemeral ice sheets in the late Eocene caused a sea-level drop and a corresponding slight increase in continental erosion, providing the nutrients necessary for high planktonic productivity. Also, an increase in deep water formation tied to ice-sheet expansion would be balanced by increased upwelling of nutrient-rich waters in other parts of the oceans. In light of the inverse relationship between $CaCO_3$ content and magnetic susceptibility, it is reasonable to imagine that marly layers were deposited during relatively wet (and possibly warm) periods with a greater fluvial influx of detrital matter. It is important to note, however, that while ice-sheet development is a global phenomenon, productivity changes in a site like the Mediterranean probably occurred on a more local scale. Cold periods, therefore, may not be equated with high productivity at other latitudes.

Stable Isotopes and Orbital Cycle Strength

The spectral power of the orbital cycles of eccentricity, obliquity, and precession varies significantly from proxy to proxy. Most notably, the $\delta^{18}O$ spectral plot for meter levels 15–20 exhibits statistically significant high-frequency precessional peaks that dwarf the other possible orbital signals. This is in stark contrast with the $\delta^{13}C$ spectral plot for the same interval, in which the low-frequency eccentricity cycle greatly exceeds the 95% confidence limit (Fig. 5). One possible explanation for these differences lies in the response times of the environmental cycles to which the proxies are tied. The $\delta^{13}C$ values of marine carbonates are linked to the global carbon cycle, which, with many reservoirs, has a slow response time (relative to the hydrologic cycle). The eccentricity cycle, then, may be amplified by the long oceanic residence time of carbon, which was similarly noted by Pälike et al. (2006) for long-period eccentricity (405 k.y.). Contrarily, the hydrologic cycle, to which the $\delta^{18}O$ values of marine carbonates are tied, is characterized by much faster relative response times and therefore may amplify precessional cycles. For example, it is believed that the African monsoon undergoes large changes in tune with the precessional cycle (e.g., Pokras and Mix, 1987; Tuenter et al., 2003).

Correlation with the Astronomical Time Scale

The spectral analysis results indicate that the Massignano sequence's rhythmic bedding reflects orbitally paced climate variations. Even though eccentricity weakly affects insulation, the prominent ~95 k.y. peak common to all four proxies (particularly in the upper section) implies that the late Eocene and early Oligocene climate experienced eccentricity forcing. Others have similarly found the eccentricity signal to be disproportionately significant as far back as the Miocene, with strength far greater than its theoretical contribution to insolation would suggest (e.g., Fischer, 1991; Clemens and Tiedemann, 1997; van Vugt et al., 2001; Cleaveland et al., 2002). This disproportional relationship of eccentricity to climate could perhaps be explained by an amplifying mechanism, such as the ice-albedo feedback (Cleaveland et al., 2002; see also DeConto et al. 2007). With Antarctic ice sheets emerging in the late Eocene (e.g., Miller et al., 1991; Zachos et al., 1992), it is conceivable that this feedback mechanism would have come into play during the deposition of the Massignano section. Alternatively, the ~95 k.y. cycle may not represent the direct effect of eccentricity on insolation, but the modulation of the precessional amplitude by eccentricity.

We achieved an astronomical correlation between Laskar's eccentricity curve and Massignano's smoothed magnetic susceptibility and calcium carbonate data (Fig. 10) through pattern matching constrained by the dated volcanic ashes at meter levels 7.2, 12.7, and 14.7. Following Cleaveland et al. (2002), eccentricity highs were matched with magnetic susceptibility highs and carbonate content lows. For pattern matching, we used the smoothed magnetic susceptibility data from the entire Massignano section (meters 0.5–23). Of all four proxies, the magnetic susceptibility data exhibit the least amount of noise, and Milankovitch peaks rise above the 95% confidence level in both the whole-section and lower-section spectral plots (Figs. 4 and 6). In order to confirm the validity of the match, we similarly matched the smoothed $CaCO_3$ content data from the upper portion of the sequence to Laskar eccentricity and found the two correlations to be in agreement (Fig. 11). The correlation yields a refined date for the Eocene-Oligocene boundary of 33.91 ± 0.05 Ma, which is just 0.2 m.y. older than the previously proposed date of 33.7 ± 0.4 Ma (Montanari et al., 1988). Precise ages of 35.13 ± 0.05 Ma, 34.55 ± 0.05 Ma, and 34.32 ± 0.05 Ma are also obtained for the three radioisotopically dated volcanic ashes of at meter levels 7.2, 12.7, and 14.7, respectively. All three precise ages fall within the error bars of the previous radiometric dates of 35.4 ± 0.3 Ma, 34.5 ± 0.3 Ma, and 34.2 ± 0.2 Ma (Montanari et al., 1993).

These refined dates are not in agreement with the age of 33.714 Ma for the Eocene-Oligocene boundary proposed by Jovane et al. (2006). Differences may arise for the following reasons: (1) Using the Lowrie and Lanci (1994) magnetostratigraphic study at Massignano combined with numerical ages from Cande and Kent (1995), Jovane et al. (2004) established a linear sedimentation rate of ~6.9 m/m.y. for the Scaglia Variegata Formation, which they subsequently applied to the whole of the Massignano section (both the Scaglia Variegata and Scaglia Cinerea Formations); and (2) Jovane et al. (2006) started their tuning with a visual match for the 400 k.y. eccentricity cycle and subsequently tuned their records to obliquity. While the La2004 numerical solution is accurate for eccentricity over the last

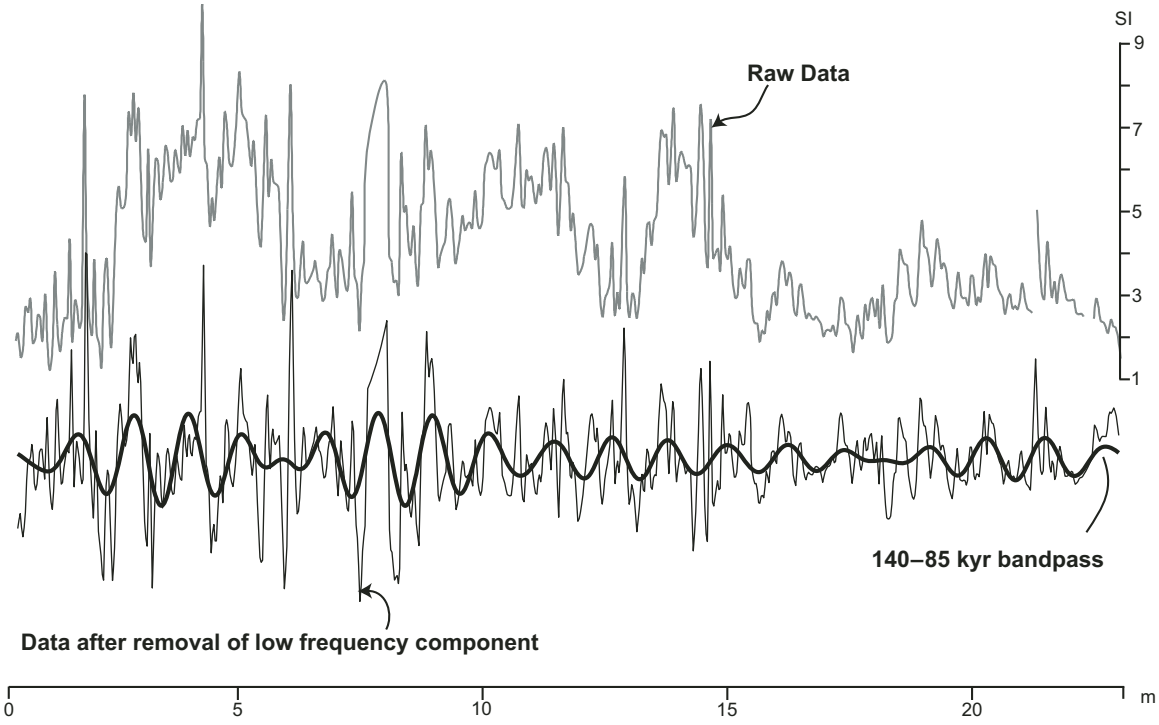

Figure 10. Massignano magnetic susceptibility proxy data shown adjacent to a version of the data with the low-frequency component removed and overlain by a smoothed version of the raw data (45–140 k.y. band-pass filter).

40 m.y., this is not necessarily the case for precession and obliquity, as they are dependent on the Earth-Moon system in addition to the orbital part of the solution (Hilgen et al., 2006; see also Pälike et al., 2004).

Impacts, Comet/Asteroid Showers, and Climate Cycles

While we and others (e.g., Jovane et al., 2006) have shown that some portions of the Massignano section preserve a clear record of Milankovitch orbital cycles, it is also true that the signatures of impact events (and a comet/asteroid shower) are prevalent in parts of the section, allowing us to explore the question of whether or not extraterrestrial events can alter the preservation of "normal" Milankovitch cycles. The lower portion of the outcrop contains evidence of at least two, possibly three, extraterrestrial impacts, including the giant Popigai and Chesapeake Bay impact events (Montanari and Koeberl, 2000; Bodiselitsch et al., 2004; Glass et al., 2004). The Popigai impact crater, a 100-km-diameter structure located in Siberia, Russia, has been dated at 35.7 ± 0.8 Ma, and the 85-km-diameter Chesapeake Bay impact crater is indistinguishable in age (e.g., Bottomley et al., 1997; Koeberl et al., 1996). Evidence of these events has been reported in numerous other early late Eocene sedimentary successions (e.g., Glass et al., 1985; Koeberl and Glass, 1988; see also review in Koeberl, this volume). At Massignano, an impactoclastic layer at ~5.6 m is marked by an iridium anomaly (Montanari et al., 1993), shocked quartz (Clymer et al., 1996; Langenhorst, 1996), extraterrestrial Ni-rich spinel and altered microkrystites (Pierrard et al., 1998), and, finally, a ^{3}He anomaly (Farley et al., 1998). Impactoclastic layers at meter levels 6.19 and 10.25 are similarly distinguished by ^{3}He anomalies, as well as increased iridium abundances (Bodiselitsch et al., 2004). The ^{3}He anomaly at Massignano is in fact quite broad, spanning from about meter level 2 to 15, with its maximum value coincident with the Ir anomaly at 5.6 m (Farley et al., 1998). Farley et al. (1998) argued that this ^{3}He enhancement is attributable to an early late Eocene comet shower lasting ~2.2 m.y. In contrast, Tagle and Claeys (2004) suggested that the increase in delivery of interplanetary dust particles (IDPs) implied by the ^{3}He anomaly could instead be explained by an asteroid shower.

Both individual impact events and comet/asteroid showers have the potential to affect global climate. An impact occurring on a continental shelf, such as the Chesapeake Bay impact (e.g., Koeberl et al., 1996; Poag et al., 2004), might be coupled with the release of methane hydrates, and certainly would deliver a significant amount of water vapor into the atmosphere, both of which contribute to the greenhouse effect and induce global warming, besides changing the Earth's albedo. A terrestrial impact, such as the Popigai impact event (e.g., Bottomley et al., 1997; Tagle and Claeys, 2005), on the other hand, can be linked to global cooling and a corresponding decrease in bioproductivity (Toon et al., 1997). Global cooling could also be attributed to the dust-particle loading of the atmosphere associated with the increased levels of planetary dust inherent to a comet shower. At Massignano,

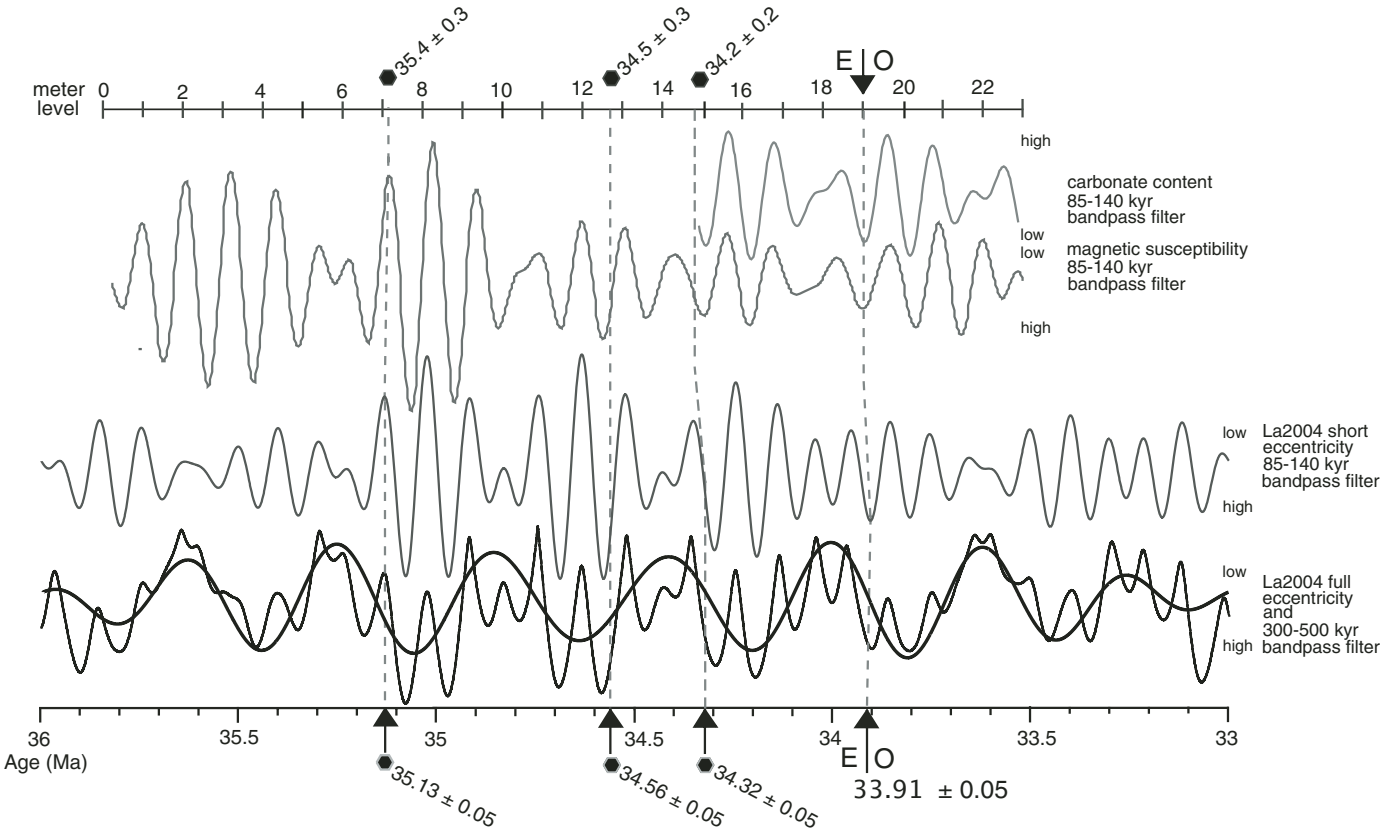

Figure 11. Correlations between Laskar full eccentricity, Laskar short eccentricity (85–140 k.y. band-pass), Massignano magnetic susceptibility, and Massignano carbonate content. Both the magnetic susceptibility data and the $CaCO_3$ content have been smoothed by a 85–140 k.y. band-pass filter to isolate the short eccentricity signal. The filtered curves overlie the raw magnetic susceptibility and $CaCO_3$ data, shown in light gray. Pattern matching constrained by the three volcanic ashes yields a date for the Eocene-Oligocene boundary of 33.91 ± 0.05 Ma, somewhat older than the previously determined date of 33.7 ± 0.4 (Montanari et al., 1988). The smoothed $CaCO_3$ data confirm the pattern match made with the smoothed magnetic susceptibility curve. E—Eocene; O—Oligocene.

based on stable isotope variations, Bodiselitsch et al. (2004) proposed that impact-induced warm pulses punctuate the general trend of continuous Eocene-Oligocene cooling. Vonhof et al. (2000) similarly used stable isotope records from Maud Rise to suggest that late Eocene impact events (ca. 35.5 Ma) accelerated the long-term cooling trend. Because the biotic response to the impacts was greater than would be expected, Vonhof et al. (2000) invoked the possibility of a feedback mechanism, such as the ice-albedo feedback, which could have prolonged the duration of impact-induced climate cooling. The ice-albedo feedback has also been shown to be modulated by Milankovitch periodicities (see Muller and MacDonald, 2000, and references therein); however, it is possible that the climate alterations caused by the impact events could overprint or swamp the longer-term climate cycling events paced by orbital cycles.

The $CaCO_3$ content and magnetic susceptibility sliding-window plots from the Massignano section (Figs. 12 and 13) indicate that the record of Milankovitch cyclicity, while persistent throughout the section, changes during and immediately following extraterrestrial events. In the $CaCO_3$ plot with a 50–10 k.y. band-pass filter, beginning at a window midpoint of ~5.6 m and extending to ~13 m, the relative strength of the obliquity signal is masked by stronger power in some discontinuous 26–30 k.y. cycles. A similar, though less pronounced pattern of discontinuous, stronger-power 30–36 k.y. cycles is visible in the 50–10 k.y. band-pass filter magnetic susceptibility plot, again beginning at a window midpoint of ~5.6 m and extending to ~12–13 m. Most remarkably, the onset of this pattern is coincident with the Ir anomaly and shocked-quartz layer at meter level 5.6. The disruption is also probably at least partially coupled to the ongoing comet/asteroid shower extending from about meter level 2 to 15.

Possible causes for the masked record of Milankovitch cycles include both global and regional mechanisms. Global mechanisms for impact-related climatic changes include the ice-albedo feedback or impact-related atmospheric alterations combined with ongoing interplanetary dust particle input associated with the comet or asteroid shower. On a more regional scale, the record of Milankovitch cycles could be altered by changes in the rate of sedimentation on a time scale comparable to the Milankovitch cycles.

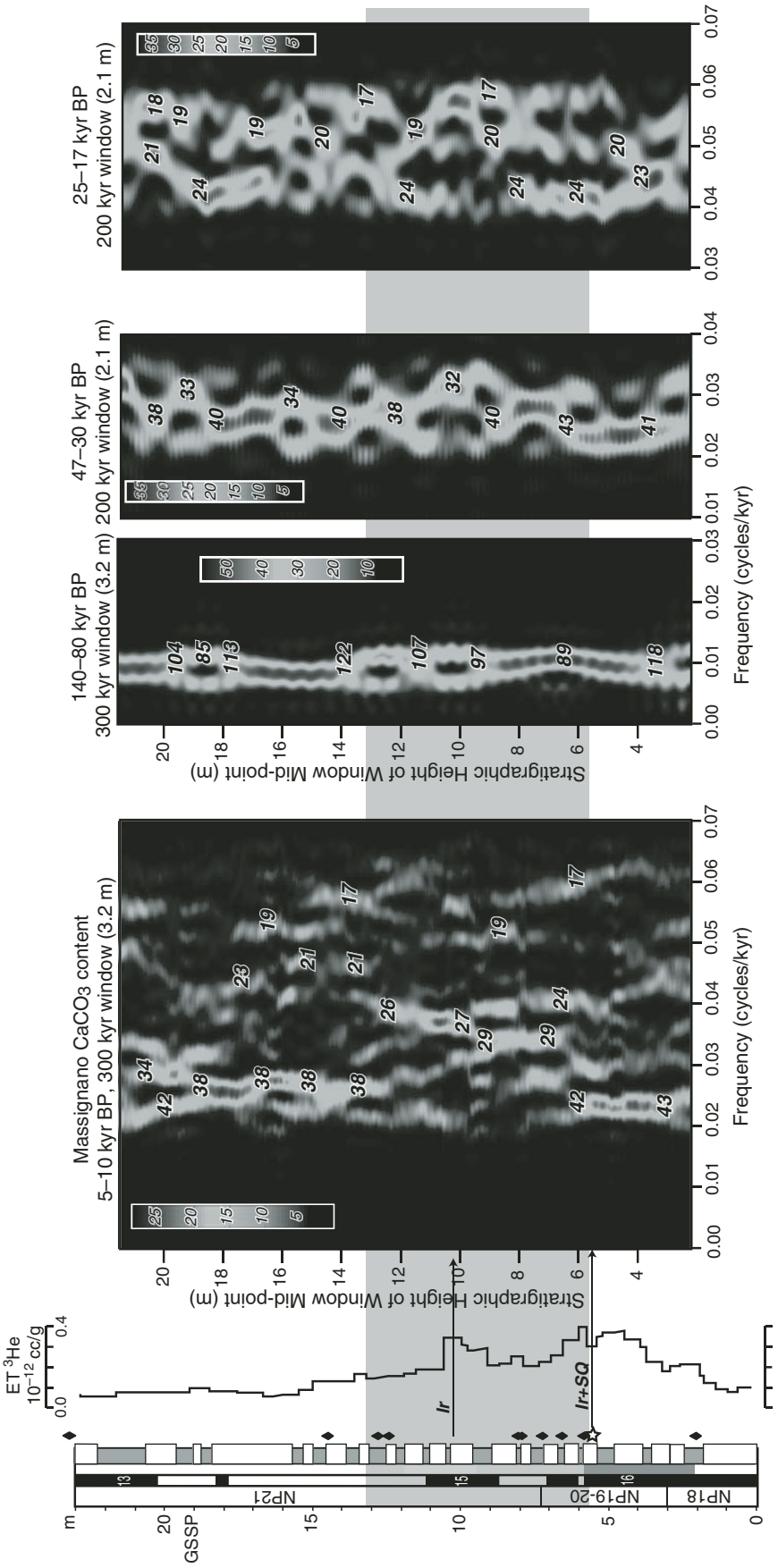

Figure 12. Evolutionary spectral analysis results from the whole-section $CaCO_3$ data. BP stands for band-pass filter. Milankovitch cycles persist through the zone of the comet shower; however, the relative strength of the obliquity signal is masked by stronger power in some discontinuous 26–30 k.y. cycles. The onset of this zone is the Ir anomaly and shocked-quartz layer at meter level 5.6. GSSP—global stratotype section and point.

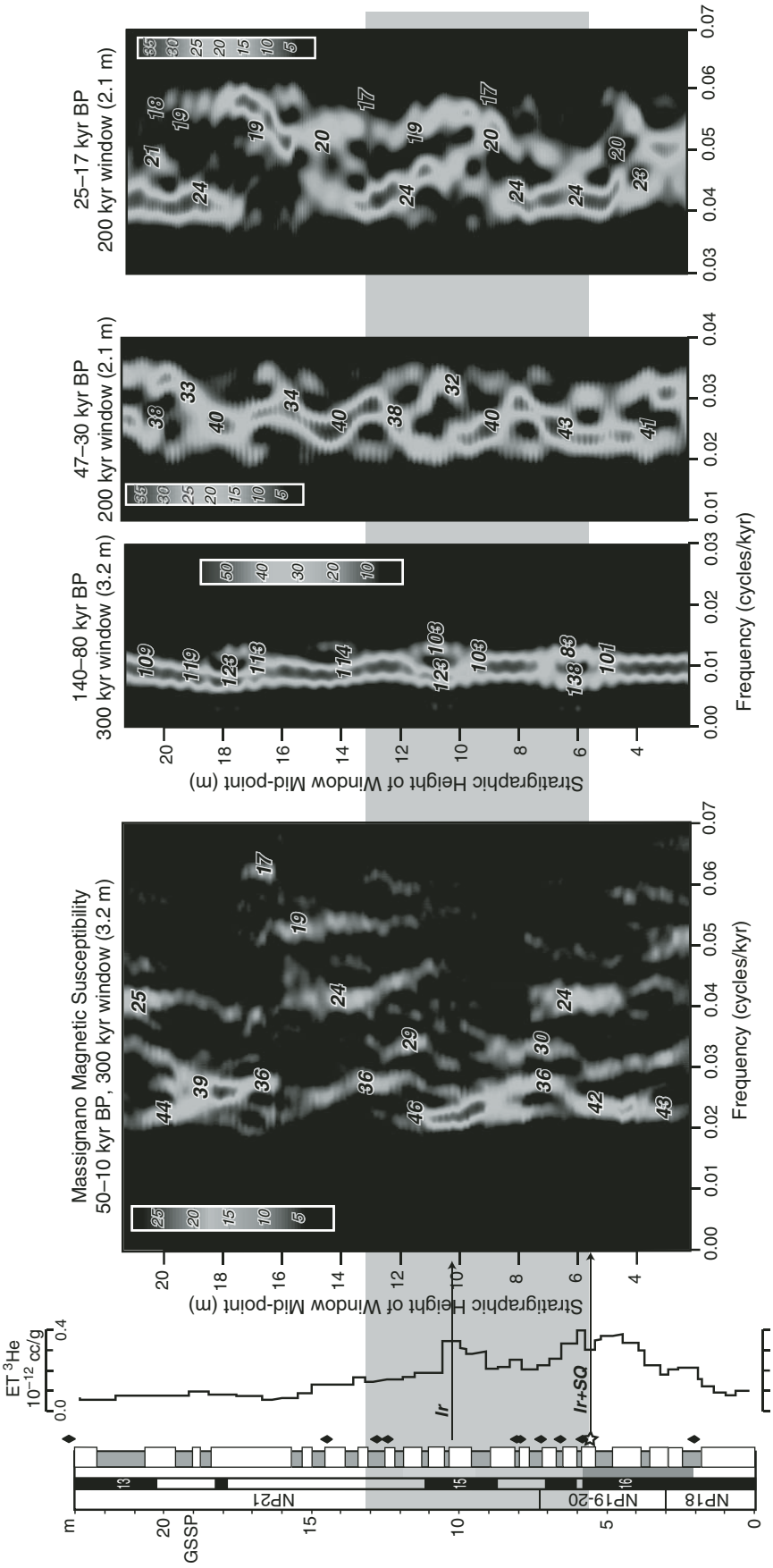

Figure 13. Evolutionary spectral analysis results from the whole-section magnetic susceptibility data. BP stands for band-pass filter. Milankovitch cycles similarly seem to persist through the zone of the comet/asteroid shower; however, the relative strength of the obliquity signal is once again masked by stronger power in some discontinuous 26–30 k.y. cycles, beginning at the 5.6 m Ir anomaly. GSSP—global stratotype section and point.

Certainly, disruptions in the sliding-window plots can in part be attributable to changes in sedimentation rate; some of the lateral oscillations of Milankovitch peaks in the plots are indicative of this. If we were to apply a different linear sedimentation rate to the section, the relative positions and powers of the peaks would not change; rather only the frequencies correlated to the peaks. Trying to vary sedimentation rate over time in a more complex fashion is difficult to justify, as sedimentation rates are difficult to constrain at such a fine resolution. Furthermore, changes in sedimentation rate do not preclude extraterrestrial disruptions, as changes could and likely would be caused by these events.

While it is intriguing that extraterrestrial events appear to have affected global climate on longer time scales, questions remain. Milankovitch forcing is certainly obscured in the $CaCO_3$, $\delta^{18}O$, and $\delta^{13}C$ proxy records of the lower Massignano section, but the magnetic susceptibility record emerges largely unscathed. It is curious that this particular proxy would be less susceptible to impact-related climatic overprinting than the other proxies. Perhaps the usual fluvial or wind-deposited detrital influx is augmented by the slowly accreting extraterrestrial dust, preserving some level of cyclicity. Despite lingering questions, it is reasonable to assert that impact-related climatic changes interacted with the continuous record of longer-term Milankovitch cycles in such a way that they were disrupted or obscured during the deposition of Eocene sediments at Massignano.

CONCLUSIONS

Spectral analyses of four high-resolution climate proxies indicate that deposition at Massignano was orbitally controlled. The relationship between these proxies, where stable isotope highs correspond to calcium carbonate highs and magnetic susceptibility lows, helps to elucidate the paleoclimatic conditions imposed by orbital forcing. Marly limestones are inferred to represent wet/warm periods, while limestones represent dry/cold periods characterized by enhanced productivity. By means of pattern matching, we are able correlate the presumed eccentricity signal in the Massignano magnetic susceptibility and calcium carbonate data to La2004, providing astronomical ages for the entire section. This correlation yields a refined date for the Eocene-Oligocene boundary of 33.91 ± 0.05 Ma.

While Milankovitch cyclicity is persistent throughout the section, the record of this cyclicity changes in the lower portion of the outcrop, which contains three possible impact events and a ^3He anomaly indicative of a comet/asteroid shower ~2.2 m.y. in duration. Climate alterations caused by these extraterrestrial events were most likely exaggerated such that Milankovitch forcing was overprinted and obscured. Possible mechanisms for the exaggeration of impact-related climatic changes include: (1) on a more regional scale, changes in sedimentation rate on a time scale comparable to Milankovitch cycles; or (2) more globally, the ice-albedo feedback or a combination of ongoing atmospheric dust-particle loading with impact-related atmospheric alterations. We encourage analyses of other climate records of this age in order to establish the extent of this phenomenon.

ACKNOWLEDGMENTS

We thank Laura Cleaveland and Alessandro Grippo for their thoughtful reviews as well as Frits Hilgen and Rodolfo Coccioni for additional helpful comments, all of which helped to improve this paper. This work was supported by the Coldigioco Research Fund (Montanari and Bice), the Carleton College Duncan Stewart Fellowship (Brown), and by the Austrian Science Foundation FWF, project P18862-N10 (Koeberl).

REFERENCES CITED

Banner, J.L., and Hanson, G.N., 1990, Calculation of simultaneous isotopic and trace element variations during water-rock interaction with applications to carbonate diagenesis: Geochimica et Cosmochimica Acta, v. 54, p. 3123–3137, doi: 10.1016/0016-7037(90)90128-8.

Berggren, W.A., and Prothero, D.R., 1992, Eocene-Oligocene Climatic and Biotic Evolution: Princeton, New Jersey, Princeton University Press, 568 p.

Bickert, T., 2000, Influence of geochemical processes on stable isotope distribution in marine sediments, *in* Schulz, H.D., and Zabel, M., eds., Marine Geochemistry: Berlin, Springer, p. 309–333.

Bodiselitsch, B., Montanari, A., Koeberl, C., and Coccioni, R., 2004, Delayed climate cooling in the late Eocene caused by multiple impacts: High-resolution geochemical studies at Massignano, Italy: Earth and Planetary Science Letters, v. 223, p. 283–302, doi: 10.1016/j.epsl.2004.04.028.

Bottomley, R., Grieve, R., York, D., and Masaitis, V., 1997, The age of the Popigai impact event and its relation to events at the Eocene/Oligocene boundary: Nature, v. 388, p. 365–368, doi: 10.1038/41073.

Cande, S.C., and Kent, D.V., 1995, Revised calibration of the geomagnetic polarity timescale for the Late Cretaceous and Cenozoic: Journal of Geophysical Research, v. 100, p. 6093–6095, doi: 10.1029/94JB03098.

Cleaveland, L.C., Jensen, J., Goese, S., Bice, D.M., and Montanari, A., 2002, Cyclostratigraphic analysis of pelagic carbonates at Monte dei Corvi (Ancona, Italy) and astronomical correlation of the Serravallian-Tortonian boundary: Geology, v. 30, p. 931–934, doi: 10.1130/0091-7613(2002)030<0931:CAOPCA>2.0.CO;2.

Clemens, S.C., and Tiedemann, R., 1997, Eccentricity forcing of Pliocene–early Pleistocene climate revealed in a marine oxygen-isotope record: Nature, v. 385, p. 801–804, doi: 10.1038/385801a0.

Clymer, A.K., Bice, D.M., and Montanari, A., 1996, Shocked quartz in the late Eocene: Impact evidence from Massignano, Italy: Geology, v. 24, p. 483–486, doi: 10.1130/0091-7613(1996)024<0483:SQFTLE>2.3.CO;2.

Coccioni, R., and Galeotti, S., 2003, Deep-water foraminiferal events from the Massignano Eocene/Oligocene boundary stratotype, central Italy, *in* Prothero, D.R., Ivany, L.C., and Nesbitt, E.A., eds., From Greenhouse to Icehouse: The Marine Eocene-Oligocene Transition: New York, Columbia University Press, p. 438–452.

Coccioni, R., Monaco, P., Monechi, S., Nocchi, M., and Parisi, G., 1988, Biostratigraphy of the Eocene-Oligocene boundary at Massignano (Ancona, Italy), *in* Premoli-Silva, I., Coccioni, R., and Montanari, A., eds., The Eocene-Oligocene Boundary in the Marche-Umbria Basin (Italy): Ancona, Italy, International Union of Geological Sciences, p. 59–80.

Cotillion, P., 1995, Constraints for using high-frequency sedimentary cycles in cyclostratigraphy, *in* House, M.R., and Gale, A.S., eds., Orbital Forcing Timescales and Cyclostratigraphy: Geological Society of London Special Publication 85, p. 133–141.

Coxall, H.K., Wilson, P.A., Pälike, H., Lear, C.H., and Backman, J., 2005, Rapid stepwise onset of Antarctic glaciation and deeper calcite compensation in the Pacific Ocean: Nature, v. 433, p. 53–57, doi: 10.1038/nature03135.

Crick, R.E., Ellwood, B.B., Hassani, A.E., Feist, R., and Hladil, J., 1997, Magnetosusceptibility event and cyclostratigraphy (MSEC) of the Eifelian-Givetian GSSP and associated boundary sequences in North Africa and Europe: Episodes, v. 20, p. 167–174.

DeConto, R., Pollard, D., and Harwood, D., 2007, Sea ice feedback and Cenozoic evolution of Antarctic climate and ice sheets: Paleoceanography, v. 22, PA3214, doi: 10.1029/2006PA001350, 18 p.

Dercourt, J., Ricou, L.E., and Vrielynck, B., eds., 1993, Atlas Tethys Palaeoenvironmental Maps: Paris, Gauthier Villars, 307 p.

Deutsch, A., and Koeberl, C., 2006, Establishing the link between the Chesapeake Bay impact structure and the North American tektite strewn field: The Sr-Nd isotopic evidence: Meteoritics & Planetary Science, v. 41, p. 689–703.

Einsele, G., and Ricken, W., 1991, Limestone-marl alteration—An overview, *in* Einsele, G., Ricken, W., and Seilacher, A., eds., Cycles and Events in Stratigraphy: Berlin, Springer-Verlag, p. 23–47.

Ellwood, B.B., Crick, R.E., El Hassani, A., Benoist, S.L., and Young, R.H., 2000, Magnetosusceptibility event and cyclostratigraphy method applied to marine rocks: Detrital input versus carbonate productivity: Geology, v. 28, p. 1135–1138, doi: 10.1130/0091-7613(2000)28<1135:MEACMA>2.0.CO;2.

Farley, K.A., Montanari, A., Shoemaker, E.M., and Shoemaker, C.S., 1998, Geochemical evidence for a comet shower in the late Eocene: Science, v. 280, p. 1250–1253, doi: 10.1126/science.280.5367.1250.

Fischer, A.G., 1991, Orbital cyclicity in Mesozoic strata, *in* Einsele, G., Ricken, W., and Seilacher, A., eds., Cycles and Events in Stratigraphy: Berlin, Springer-Verlag, p. 48–62.

Glass, B.P., and Koeberl, C., 1999, Ocean Drilling Project Hole 689B spherules and upper Eocene microtektites and clinopyroxene-bearing spherule strewn fields: Meteoritics & Planetary Science, v. 34, p. 185–196.

Glass, B.P., Burns, C.A., Crosbie, J.R., and DuBois, D.L., 1985, Late Eocene North American microtektites and clinopyroxene-bearing spherules: Journal of Geophysical Research, v. 90, p. D175–D196.

Glass, B.P., Liu, S.B., and Montanari, A., 2004, Impact ejecta in upper Eocene deposits at Massignano, Italy: Meteoritics & Planetary Science, v. 39, p. 589–597.

Grippo, A., Fischer, A.G., Hinnov, L.A., Herbert, T.D., and Premoli-Silva, I., 2004, Cyclostratigraphy and chronology of the Albian stage (Italy), *in* D'Argenio, B., Fischer, A.G., Premoli-Silva, I., Weissert, H., and Ferreri, V., eds., Cyclostratigraphy: Approaches and Case Histories: Society for Sedimentary Geology Special Publication 81, p. 57–81.

Hilgen, F., Brinkhuis, H., and Zachariasse, W.J., 2006, Unit stratotypes for global stages: The Neogene perspective: Earth-Science Reviews, v. 74, p. 113–125.

Huber, H., Koeberl, C., King, D.T., Petruni, L.W., and Montanari, A., 2001, Effects of bioturbation through the late Eocene impactoclastic layer near Massignano, Italy, *in* Buffetaut, E., and Koeberl, C., eds., Geological and Biological Effects of Impact Events, Impact Studies: Berlin, Springer Verlag, p. 197–216.

Jovane, L., Florindo, F., Dinares-Turell, J., and Turrell, S., 2004, Environmental magnetic record of paleoclimate change from the Eocene-Oligocene stratotype section, Massignano, Italy: Geophysical Research Letters, v. 31, p. L15601, doi: 10.1029/2004GL020554, 4 p.

Jovane, L., Florindo, F., Sprovieri, M., and Pälike, H., 2006, Astronomic calibration of the late Eocene/early Oligocene Massignano section (central Italy): Geochemistry, Geophysics, Geosystems, v. 7, doi: 10.1029/2005GC001195, 10 p.

Jovane, L., Sprovieri, M., Florindo, F., Acton, G., Coccioni, R., Dall'Antonia, B., and Dinarès-Turrell, J., 2007, Eocene-Oligocene paleoceanographic changes in the stratotype section, Massignano, Italy: Clues from rock magnetism and stable isotopes: Journal of Geophysical Research, v. 112, B11101, doi: 10.1029/2007JB004963, 16 p.

Koeberl, C., and Glass, B.P., 1988, Chemical composition of North American microtektites and tektite fragments from Barbados and DSDP Site 612 on the continental slope off New Jersey: Earth and Planetary Science Letters, v. 87, p. 286–292, doi: 10.1016/0012-821X(88)90016-7.

Koeberl, C., Poag, C.W., Reimold, W.U., and Brandt, D., 1996, Impact origin of Chesapeake Bay structure and the source of North American tektites: Science, v. 271, p. 1263–1266, doi: 10.1126/science.271.5253.1263.

Kuiper, K.F., Deino, A., Hilgen, F.J., Krijgsman, W., Renne, P.R., and Wijbrans, J.R., 2008, Synchronizing rock clocks of Earth history: Science, v. 320, p. 500–504, doi: 10.1126/science.1154339.

Langenhorst, F., 1996, Characteristics of shocked quartz in late Eocene impact ejecta from Massignano (Ancona, Italy): Clues to shock conditions and source crater: Geology, v. 24, p. 487–490, doi: 10.1130/0091-7613(1996)024<0487:COSQIL>2.3.CO;2.

Laskar, J., 1999, The limits of Earth orbital calculations for geological time scale use: Philosophical Transactions of the Royal Society of London, v. 357, p. 1735–1759.

Laskar, J., Robutel, P., Joutel, F., Gastineau, M., Correia, A.C.M., and Levrard, B., 2004, A long-term numerical solution for the insolation quantities of the Earth: Astronomy & Astrophysics, v. 428, p. 261–285, doi: 10.1051/0004-6361:20041335.

Lourens, L.J., and Hilgen, F.J., 1997, Long-periodic variations in the Earth's obliquity and their relation to third-order eustatic cycles and late Neogene glaciations: Quaternary International, v. 40, p. 43–52, doi: 10.1016/S1040-6182(96)00060-2.

Lowrie, W., and Lanci, L., 1994, Magnetostratigraphy of Eocene-Oligocene boundary sections in Italy: No evidence for short subchrons within chrons 12R and 13R: Earth and Planetary Science Letters, v. 126, p. 247–258, doi: 10.1016/0012-821X(94)90110-4.

Mackensen, A., and Ehrmann, W.U., 1992, Middle Eocene through early Oligocene climate history and paleoceanography in the Southern Ocean: Stable oxygen and carbon isotopes from ODP Sites on Maud Rise and Kerguelen Plateau: Marine Geology, v. 108, p. 1–27, doi: 10.1016/0025-3227(92)90210-9.

Mader, D., Cleaveland, L.C., Bice, D.M., Montanari, A., and Koeberl, C., 2004, High-resolution cyclostratigraphic analysis of multiple climate proxies from a short Langhian pelagic succession in the Conero Riviera, Ancona (Italy): Palaeogeography, Palaeoclimatology, Palaeoecology, v. 211, p. 325–344, doi: 10.1016/j.palaeo.2004.06.001.

Miller, K.G., Wright, J.D., and Fairbanks, R.G., 1991, Unlocking the ice house: Oligocene-Miocene oxygen isotopes, eustasy, and margin erosion: Journal of Geophysical Research, v. 96, p. 6829–6848, doi: 10.1029/90JB02015.

Miller, K.G., Browning, J.V., Aubry, M.P., Wade, B.S., Katz, M.E., Kulpecz, A.A., and Wright, J.D., 2008, Eocene-Oligocene global climate and sea-level changes: St. Stephens Quarry, Alabama: Geological Society of America Bulletin, v. 120, p. 34–53.

Mitchell, R.N., Bice, D.M., Montanari, A., Cleaveland, L.C., Christianson, K.T., Coccioni, R., and Hinnov, L.A., 2008, Oceanic anoxic cycles? Orbital prelude to the Bonarelli Level (OAE 2): Earth and Planetary Science Letters, v. 267, p. 1–16, doi: 10.1016/j.epsl.2007.11.026.

Mix, A.C., Le, J., and Shackleton, N.J., 1995, Benthic foraminiferal stable isotope stratigraphy of Site 846: 0–1.8 Ma, *in* Pisias, N.G., Mayer, L.A., Janecek, T.R., Palmer-Julson, A., and van Andel, T. H., et al., Proceedings of the Ocean Drilling Program, Scientific Results, Volume 138: College Station, Texas, Ocean Drilling Program, p. 839–856.

Montanari, A., and Koeberl, C., 2000, Impact Stratigraphy: The Italian Record, Lecture Notes in Earth Sciences: Berlin, Springer-Verlag, 364 p.

Montanari, A., Deino, A.L., Drake, R.E., Turrin, B.D., DePaolo, D.J., Odin, G.S., Curtis, G.H., Alvarez, W., and Bice, D.M., 1988, Radioisotopic dating of the Eocene-Oligocene boundary in the pelagic sequence of the northeastern Apennines, *in* Premoli-Silva, I., Coccioni, R., and Montanari, A., eds., The Eocene-Oligocene Boundary in the Marche-Umbria Basin (Italy): Ancona, Italy, International Union of Geological Sciences, p. 195–208.

Montanari, A., Asaro, F., Kennett, J.P., and Michel, E., 1993, Iridium anomalies of late Eocene age at Massignano (Italy), and in ODP Site 689B (Maud Rise, Antarctica): Palaios, v. 8, p. 420–437, doi: 10.2307/3515017.

Muller, R.A., and MacDonald, G.J., 2000, Ice Ages and Astronomical Causes: Data, Spectral Analysis and Mechanisms: Chichester, Praxis Publishing Ltd., 318 p.

Odin, G.S., Clauser, S., and Renard, M., 1988, Sedimentological and geochemical data on the Eocene-Oligocene boundary at Massignano (Apennines, Italy), *in* Premoli-Silva, I., Coccioni, R., and Montanari, A., eds., The Eocene-Oligocene Boundary in the Marche-Umbria Basin (Italy): Ancona, Italy, International Union of Geological Sciences, p. 175–186.

Pälike, H., Shackleton, N.J., and Röhl, U., 2001, Astronomical forcing in late Eocene marine sediments: Earth and Planetary Science Letters, v. 193, p. 589–602, doi: 10.1016/S0012-821X(01)00501-5.

Pälike, H., Laskar, J., and Shackleton, N.J., 2004, Geologic constraints on the chaotic diffusion of the solar system: Geology, v. 32, p. 929–932, doi: 10.1130/G20750.1.

Pälike, H., Norris, R.D., Herrle, J.O., Wilson, P.A., Coxall, H.K., Lear, C.H., Shackleton, N.J., Tripati, A.K., and Wade, B.S., 2006, The heartbeat of the Oligocene climate system: Science, v. 314, p. 1894–1898, doi: 10.1126/science.1133822.

Pierrard, O., Robin, E., Rocchia, R., and Montanari, A., 1998, Extraterrestrial Ni-rich spinel in Upper Eocene sediments from Massignano, Italy: Geology,

v. 26, p. 307–310, doi: 10.1130/0091-7613(1998)026<0307:ENRSIU>2.3.CO;2.

Poag, C.W., Koeberl, C., and Reimold, W.U., 2004, The Chesapeake Bay Crater: Geology and Geophysics of a Late Eocene Submarine Impact Structure: Berlin, Springer, 522 p.

Pokras, E.M., and Mix, A.C., 1987, Earth's precession cycle and Quaternary climatic change in tropical Africa: Nature, v. 326, p. 486–487, doi: 10.1038/326486a0.

Premoli-Silva, I., and Jenkins, D.J., 1993, Decision on the Eocene-Oligocene boundary stratotype: Episodes, v. 16, p. 379–381.

Premoli-Silva, I., Coccioni, R., and Montanari, A., 1988, The Eocene-Oligocene Boundary in the Marche-Umbria Basin (Italy): Ancona, Italy, International Union of Geological Sciences, 268 p.

Prothero, D.R., 1994, The Eocene-Oligocene Transition: Paradise Lost: New York, Columbia University Press, 291 p.

Schrag, D.P., DePaolo, D.J., and Richter, F.M., 1995, Reconstructing past sea-surface temperatures—correcting for diagenesis of bulk marine carbonate: Geochimica et Cosmochimica Acta, v. 59, p. 2265–2278, doi: 10.1016/0016-7037(95)00105-9.

Shackleton, N.J., Hall, M.A., and Pate, D., 1993, High-resolution stable isotope stratigraphy from bulk sediment: Paleoceanography, v. 8, p. 141–148, doi: 10.1029/93PA00123.

Stoll, H.M., and Schrag, D.P., 2000, High-resolution stable isotope records from the Upper Cretaceous rocks of Italy and Spain: Glacial episodes in a greenhouse planet?: Geological Society of America Bulletin, v. 112, p. 308–319, doi: 10.1130/0016-7606(2000)112<0308:HRSIRF>2.3.CO;2.

Tagle, R., and Claeys, P., 2004, Comet or asteroid shower in the late Eocene?: Science, v. 305, p. 492, doi: 10.1126/science.1098481.

Tagle, R., and Claeys, P., 2005, An ordinary chondrite impactor for the Popigai crater, Siberia: Geochimica et Cosmochimica Acta, v. 69, p. 2877–2889, doi: 10.1016/j.gca.2004.11.024.

Toon, O.B., Zahnle, K., Morrison, D., Turco, R.P., and Covey, C., 1997, Environmental perturbations caused by the impacts of asteroids and comets: Reviews of Geophysics, v. 35, p. 41–78, doi: 10.1029/96RG03038.

Tuenter, E., Weber, S.L., Hilgen, F.J., and Lourens, L.J., 2003, The response of the African summer monsoon to remote and local forcing due to precession and obliquity: Global and Planetary Change, v. 36, p. 219–235, doi: 10.1016/S0921-8181(02)00196-0.

Turco, E., Hilgen, F.J., Lourens, L.J., Shackleton, N.J., and Zachariasse, W.J., 2001, Punctuated evolution of global climate cooling during the late middle to early late Miocene: High-resolution planktonic foraminiferal and oxygen isotope records from the Mediterranean: Paleoceanography, v. 16, p. 405–423, doi: 10.1029/2000PA000509.

van Vugt, N., Langereis, C.G., and Hilgen, F.J., 2001, Orbital forcing in Pliocene-Pleistocene Mediterranean lacustrine deposits: Dominant expression of eccentricity versus precession: Palaeogeography, Palaeoclimatology, Palaeoecology, v. 172, p. 193–205, doi: 10.1016/S0031-0182(01)00270-X.

von Dobeneck, T., and Schmieder, F., 1999, Using rock magnetic proxy records for orbital tuning and extended time series analyses into the super- and sub- Milankovitch bands, *in* Fischer, G., and Wefer, G., eds., Use of Proxies in Paleoceanography: Examples from the South Atlantic: Berlin, Springer, p. 601–633.

Vonhof, H.B., Smit, J., Brinkhuis, H., Montanari, A., and Nederbragt, A.J., 2000, Global cooling accelerated by early late Eocene impacts?: Geology, v. 28, p. 687–690, doi: 10.1130/0091-7613(2000)28<687:GCABEL>2.0.CO;2.

Zachos, J.C., Breza, J., and Wise, S.W., 1992, Earliest Oligocene ice-sheet expansion on East Antarctica: Stable isotope and sedimentological data from Kerguelen Plateau: Geology, v. 20, p. 569–573, doi: 10.1130/0091-7613(1992)020<0569:EOISEO>2.3.CO;2.

Zachos, J.C., Stott, L.D., and Lohmann, K.C., 1994, Evolution of early Cenozoic marine temperatures: Paleoceanography, v. 9, p. 353–387, doi: 10.1029/93PA03266.

Zachos, J.C., Pagani, M., Sloan, L., Thomas, E., and Billups, K., 2001, Trends, rhythms, and aberrations in global climate 65 Ma to present: Science, v. 292, p. 686–693, doi: 10.1126/science.1059412.

Zanazzi, A., Kohn, M.J., MacFadden, B.J., and Terry, D.O., 2007, Large temperature drop across the Eocene-Oligocene transition in central North America: Nature, v. 445, p. 639–642, doi: 10.1038/nature05551.

Manuscript Accepted by the Society 16 September 2008